Geol. Bull. Univ. Peshawar, 1986, Vol. 19, pp. 121—149

PETROLOGICAL AND GEOCHEMICAL EVOLUTION OF THE KOHISTAN ARC-BATHOLITH, GILGIT, N. PAKISTAN

MICHAEL G. PETTERSON
British Geological Survey, Windsor Court, Windsor Tce,
Newcastle–on–Tyne, NE2 4HE

BRIAN F. WINDLEY
Department of Geology, University of Leicester, University Road,
Leicester, LE1 7RH.

ABSTRACT

The Kohistan batholith is the most north-westerly part of the Trans-Himalayan batholith which extends some 2700 kms from near Lhasa in the east to Pakistan in the west. Detailed fieldwork of an area of 2500 km², centred on the town of Gilgit, has shown that the batholith has evolved in three distinct stages.

(1) *An early bi-modal sequence of high-K gabbroic diorites and high SiO_2, low K tonalites, which have been deformed and folded, together with associated meta-volcanic and -sedimentary country rocks around a major syncline (the Jaglot Syncline). These early plutonics, which comprise 1/3 of the batholith, have a penetrative, gneissose fabric which is orientated parallel to the major structural trends of the area. These rocks formed in an island arc environment.*

(2) *An undeformed sequence of basic dykes, gabbros, diorites, granodiorites and granites which cut the structures associated with the Jaglot Syncline. These rocks formed in an Andean-type continental margin.*

(3) *Extensive swarms of layered aplite-pegmatite sheets, which formed after the terminal collision between India and Eurasia. Some of these rocks formed by crustal melting.*

Five rock units have yielded Rb–Sr whole rock isochron ages. These are 102 ± 12 Ma for an early, deformed, tonalite, 54 ± 4 Ma and 40 ± 6 Ma for two second stage granitoids, and 34 ± 14 Ma and 29 ± 8 Ma for two late leucogranitic sheets.

Even the least evolved gabbros of stages 1 and 2 are enriched in Rb, K, Ba, Sr, P and LREE relative to Nb, Zr, Ti, Y and HREE. With fractionation LFS/HFS, K/Na and LREE/HREE element ratios increase and the batholith displays a calc-alkaline trend with respect to Mg, Fe, Na and K. The main magmatic trend of the batholith can be explained by the fractionation of amphibole-plagioclase-magnetite ± clinopyroxene in the basic-intermediate rocks and plagioclase-K-feldspar-biotite and magnetite in the acid rocks. Zircon, apatite and sphene were important accessory minerals.

Low $^{87}Sr/^{86}Sr$ initial ratios (0.7039–0.7052) suggest that the ultimate source for the majority of the plutonics was the upper mantle. However the stage 1 tonalites and some of the stage 3 leucogranites were formed by partial melting.

INTRODUCTION

The Kohistan batholith is the most northwesterly component of the major 2700 km long Trans-Himalayan batholith which is situated north of the Indus-Zangbo suture and extends almost continuously from Afghanistan-Pakistan in the west to Burma in the east (Fig. 1). The Kohistan batholith itself extends some 280 km from the Afghanistan border in the west to Gilgit and Nanga Parbat in the east (Fig. 1). It rarely exceeds 60 km in width. The subject of this paper is a 2500 square kilometer area of the Kohistan batholith centered on the town of Gilgit at latitude 35° 58′ North and longitude 74° 27′ East (Fig. 2).

In principle, mature island arcs that form near continental margins should have some granite plutons, and active continental margins located above subduction zones should have Andean-type granitic plutons. When an island arc is accreted to a continental margin it suffers deformation and effectively becomes the leading edge of the continental plate, where it is likely to be intruded by Andean-type plutons before terminal continental collision. Such a sequence is indicated by geological relationships in the Kohistan batholith and the aim of our study is to understand its geochemical evolution from the island arc stage to the Andean stage and finally to a post-collisional stage where S–type granitic sheets were intruded. Many granitic batholiths in pre-Mesozoic collisional orogenic belts should have gone through these three stages of growth but few have been described or interpreted in this manner. The Kohistan batholith may provide a useful modern analogue for many Proterozoic and Palaeozoic batholiths.

GEOLOGICAL BACKGROUND

The geology of Kohistan has been the subject of much recent study (Coward *et al.*, 1982, 1986; Petterson and Windley, 1985; Pudsey *et al.*, 1985). Briefly the main structural units of Kohistan comprise (from north to south) :

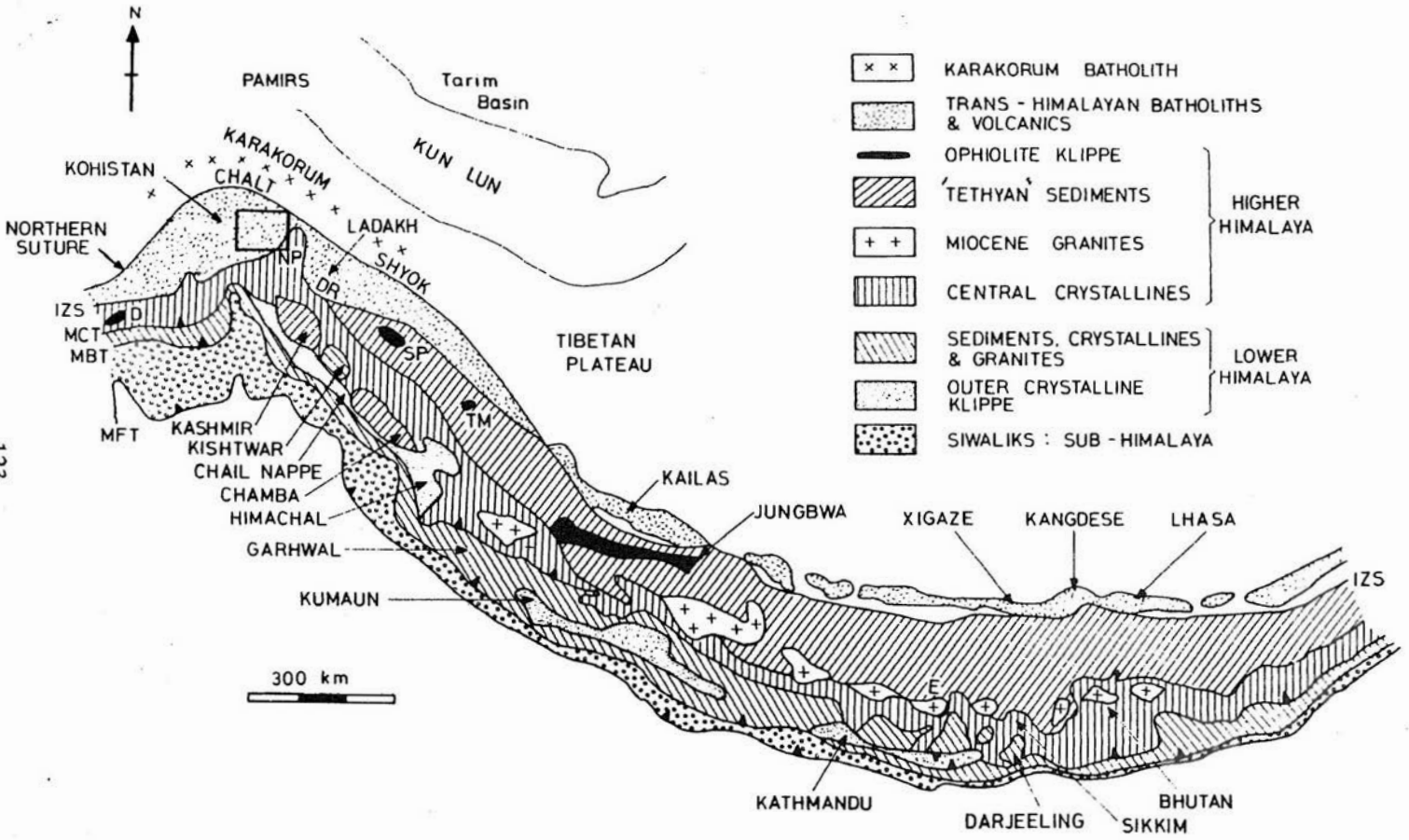

Fig. 1. Map of the Trans-Himalayan batholith showing the location of the Gilgit area in the west.

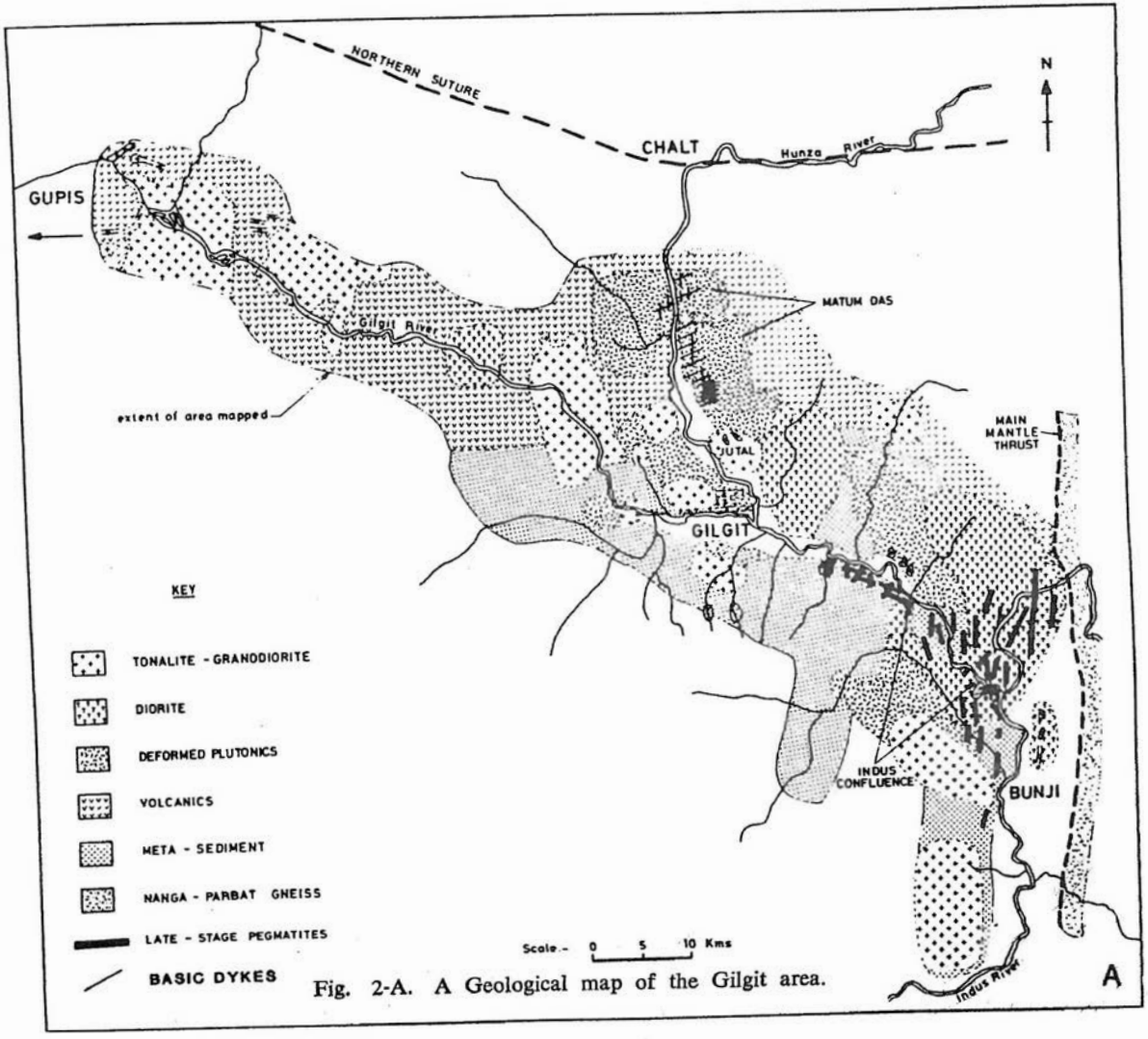

Fig. 2-A. A Geological map of the Gilgit area.

(1) The Northern Suture which separates Kohistan from the main Eurasian plate. (Pudsey *et al.*, 1985).

(2) The Yasin Group of slates, turbidites and limestones which contain Orbitolina and Rudists of Aptian/Albian age (Pudsey *et al.*, 1985).

(3) The Chalt volcanic group which consists of isoclinally folded pillow-bearing primitive island arc-type tholeiitic lavas succeeded by calc-alkaline andesites to rhyolites.

(4) The Kohistan batholith which is the subject of this paper.

(5) The Chilas Complex, originally at least 10 km thick, is a stratiform intrusion of layered norites and noritic gabbros with minor chromite-layered dunites, which has been metamorphosed to a medium-pressure granulite facies grade (Jan *et al.*, 1984). This complex probably formed in the sub-arc magma chamber.

(6) The Kamila belt – which contains many amphibolites, meta-gabbros and orthogneisses. These are probably highly deformed and metamorphosed island arc rocks.

(7) The Jijal Ultramafic Complex which comprises a sequence of hornblendites, amphibolites, garnet granulites, pyroxenites, and dunites. These are high pressure rocks metamorphosed at depth on the suture (Jan and Howie, 1981).

(8) The Indus suture which separates Kohistan from the Indian Plate.

Coward *et al.* (1982, 1986) showed that the whole Kohistan arc (including the first stage plutons of the Kohistan batholith – Petterson and Windley, 1985) was deformed by the Jaglot syncline, which is a crustal scale structure with a half wavelength of 50 km orientated east-west approximately 10 km south of Gilgit (Fig. 1). The second stage plutons of the Kohistan batholith postdate the Jaglot syncline stage of deformation.

Figure 2 shows the major subdivisions of the Kohistan batholith. A series of plutons which range in composition from hornblendite and hornblende gabbro to leucogranite intrude the Chalt meta-volcanics to the north, and meta-sediments, which include pelites, semi)pelites and psammites with minor calcareous layers, to the south. There are at least 18 separate plutons which vary in size from approximately 250 km^2 to minor stocks and bosses (Fig. 2A). The extreme relief of the area and the remarkable exposure allow complete sections of plutons to be observed – the roofs and sides of plutons can be mapped for considerable distances. The batholith is divisible into three time units.

(1) An early series of deformed plutons which are bi-modal in composition: gabbroic diorites and low-K tonalites comprise approximately equal proportions. These deformed plutons are generally medium-

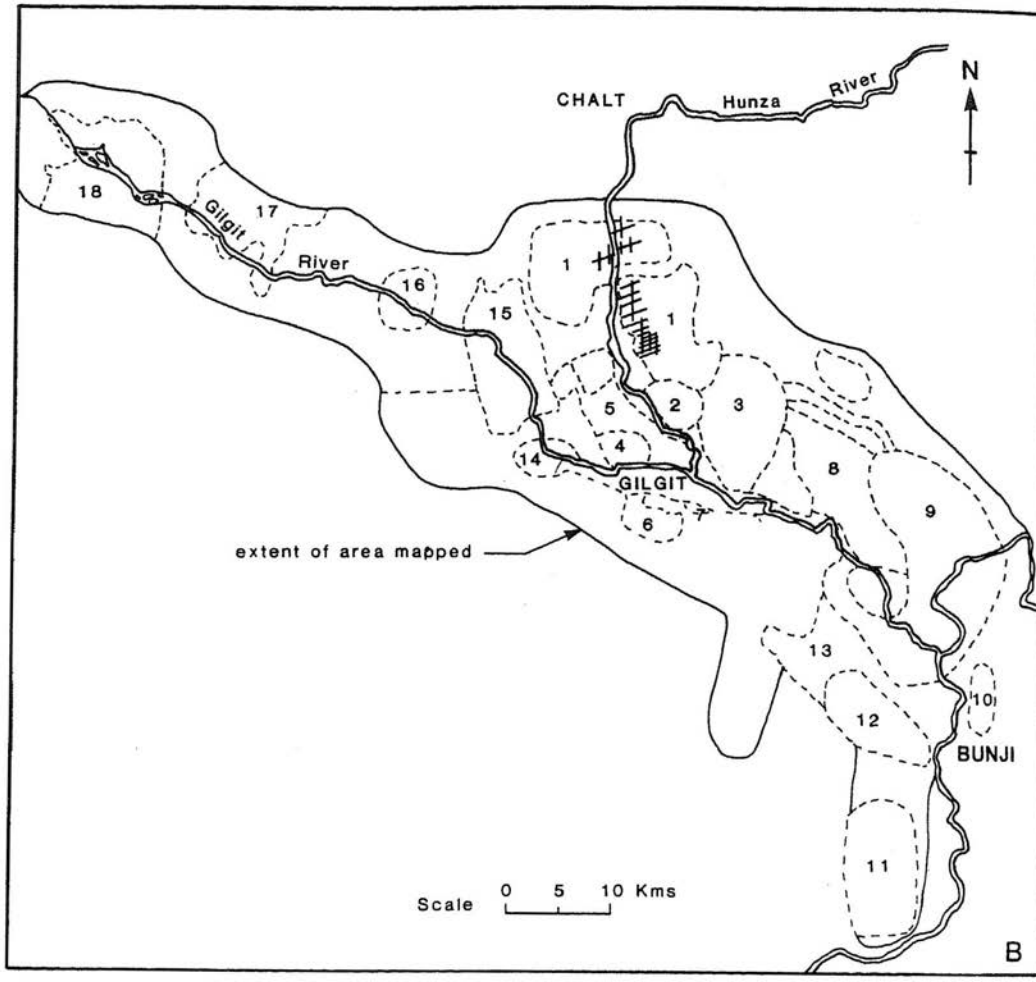

Fig. 2-B. Names of mapped plutons: (1) Matum Das (2) S. Jutal (3) Dainyar (4) Gilgit (5) North Gilgit Ridge gneiss (N.G.R.G.) (6) Jutial (7) Sakwar (8) Bagrot (9) Indus Confluence (10) Bunji (11) Thelichi (12) Jaglot (13) Gashu (14) Henzal (15) Shirot (16) Sher Kila (17) Singal (18) Gakuch.

coarse grained and are composed of hornblende, plagioclase, biotite and quartz with minor magnetite, zircon and sphene. Many amphiboles in gabbros contain relict pseudomorphs of pyroxene, now converted to amphibole. The plutons generally have a strong gneissic fabric composed of alternating melanocratic hornblende-biotite layers and leucocratic felsic layers. The strong foliation is orientated parallel to the major regional structures; i.e. they have been deformed by

the Jaglot syncline phase of deformation. The gabbroic diorite plutons contain pods and mono-mineralic layers composed almost entirely of hornblende (e.g. The North Gilgit Ridge Gneiss (N.G.R.C.) (Fig. 2)). The Matum Das tonalite pluton has a very characteristic porphyroblastic texture with porphyroblasts of quartz 7–15 mm in diameter. (Le Fort notes this in Debon *et al.*, 1987). The deformed plutons make up about one third of the plutons in the Gilgit area.

(2) A later series of undeformed plutons which cut the structures formed by the Jaglot deformation. Major plutons which range up to 250 km^2 vary from hornblende gabbro to leucogranite. Cross-cutting relationships always demonstrate that the magmatism become progressively more acidic with time : gabbros and diorites are cut by granodiorites and granites. Individual plutons may vary substantially in composition, e.g. from gabbro to leucodiorite or diorite to granite, though no plutons were observed to vary entirely from gabbro to granite. The most basic parts of any pluton occur towards its margin, thus hornblendite pods are common near the margins of basic-intermediate plutons. The rocks are generally medium-coarse grained with a granular texture, although some plutons are porphyritic with phenocrysts of hornblende or feldspar depending on their composition. Main phases are hornblende, plagioclase, biotite, quartz and alkali feldspar with accessory magnetite, zircon, apatite and sphene. Hornblende becomes modally less abundant as the rocks become more acidic in composition. Gabbros contain amphibole pseudomorphs after pyroxene. Individual outcrops are commonly very complicated, recording up to six different magmatic events. There is a major swarm of basaltic hornblende – plagioclase dykes in the Jutal-Matum Das area (Fig. 2). At their maximum concentration one dyke occurs every 10m. The dykes vary in thickness from about 2m to a few centimetres with an average of 50cm. They are fine-medium grained, and display chilled margins. Figure (3A) shows that they are orientated NE–SW to E–W. The dykes are an excellent time marker, because they cut the older deformed plutons and the structures associated with the Jaglot syncline.

(3) Most plutons are cut by aplitic-pegmatitic leucogranite sheets — commonly representing the final most-evolved liquid produced by fractionation, but there is a major swarm of leucogranitic sheets unrelated to any exposed pluton near the Indus Confluence (Fig. 2). Cross-cutting relationships show that these sheets represent the last phase of magmatism of the batholith. They vary in thickness from a few centimetres to several tens of metres with an average of 1m. They mostly have a shallow dip and a N–S strike (Fig. 3B), though locally there is a complex network of cross-cutting sheets. In places

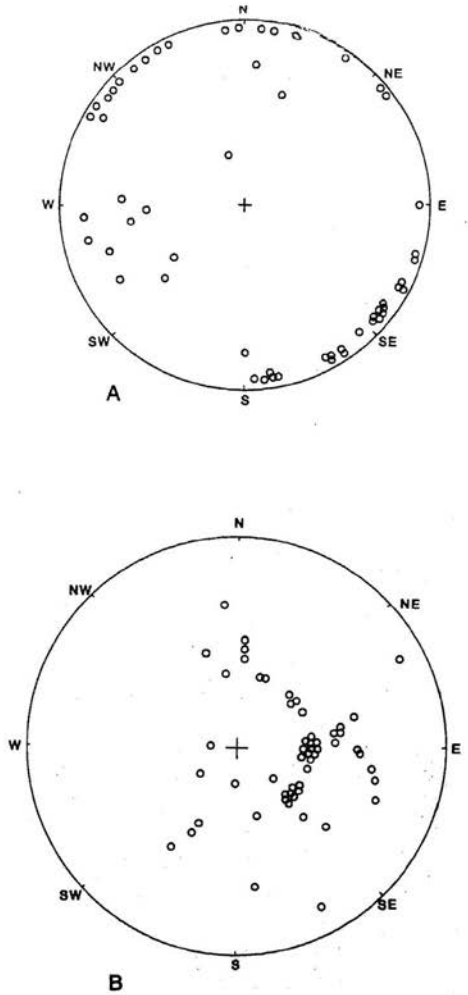

Fig. 3-A. Stereogram of poles to basic dykes around Jutal and Matum Das.
3-B. Stereogram of poles to acid sheets around the Indus Confluence.

they comprise 30–50% of exposures. Internally they are made up of alternating layers of aplite and pegmatite with up to six alternating layers in one sheet. Aplitic layers have an average grain size of 2mm, whilst pegmatite layers contain megacrysts of feldspar and biotite up to 30cm long. Biotite, quartz, feldspar and tourmaline are the major minerals, often forming mono-mineralic layers. Mafic minerals generally comprise about 7% of the sheets. Garnet and muscovite occur in some sheets which intrude sediments 10 km S.E. of Gilgit (the Parri acid sheets in Petterson and Windley, 1985).

TABLE 1. GEOLOGICAL HISTORY OF THE KOHISTAN BATHOLITH AND THE RELATIVE PROPORTION OF THE MAJOR ROCK UNITS.

Event	Time (Ma)	Comment
Intrusion of an early bi-modal series of gabbros, diorites and tonalites, deformed by the Jaglot syncline phase of deformation.	102 ± 12	Isochron produced from Matum Das tonalite pluton.
Jaglot syncline phase of deformation.		
Intrusion of basic dykes north of Gilgit.	75 Ma	Predominant NE-SW orientation of dyke swarm.
Gabbro-diorite intrusions.	?70–?50	65 ± 2 Ma-Dainyar Diorite (D. Rex — in Petterson *et al.*, in prep).
Granodioritic-granitic intrusions.	54 ± 4 Ma 40 ± 6 Ma	Similar age ranges from other parts of the Trans-Himalayan Batholith.
Intrusion of layered aplite-pegmatite sheets.	34 ± 14 Ma 29 ± 8 Ma	Final intrusive phase.

RELATIVE PROPORTIONS OF THE MAJOR ROCK UNITS

1st Stage Tonalite Plutons	1st Stage Gabbro-Diorite	2nd Stage Gabbro-Diorite	2nd Stage Granodiorite-Granite	3rd Stage Aplite-Pegmatites	2nd Stage Basic Dykes
15%	16%	27%	39%	3%	1%

Rb–Sr whole rock dates by M.G. Petterson and K–Ar hornblende dates by D. Rex (Petterson and Windley, 1985) constrain the timing of successive magmatic events. A deformed first-stage tonalitic pluton at Matum Das (Fig. 2) has a Rb–Sr isochron age of 102 ± 12 Ma. The Jutal basic dykes have a K–Ar age of hornblende of 75 Ma. Rb–Sr isochron dates of two undeformed second-stage granitic plutons are 54 ± 4 Ma and 40 ± 6 Ma, and of two third-stage aplite-pegmatite sheets are 34 ± 14 Ma and 29 ± 8 Ma. Thus the batholith evolved over a period of at least 73 Ma. Table 1 summarises the main events of the Kohistan batholith together with available age determinations. Similar ages are reported for plutonic rocks of the Karakorum, Ladakh and Kangdese batholiths respectively (Casnedi *et al.*, 1978; Brookfield and Reynolds, 1981; Reynolds *et al.*, 1983; Honegger *et al.*, 1982; Maluski *et al.*, 1982; Searle, 1983; Scharer *et al.*, 1984).

ANALYTICAL TECHNIQUES

All samples were crushed to a fine powder (60mm) in an agate TEMA swingmill. Major and trace elements were determined with the Philips PW 1450 automatic XRF spectrometer at Leicester University. Trace elements were analysed from pressed-powder briquettes, whilst major elements were analysed from fused glass discs. For further details of this method see Marsh *et al.* (1980, 1983).

The Rare Earth Elements were group-separated from powdered whole rock samples using standard dissolution and cation exchange techniques at Leicester University, and analysed with the inductively coupled plasma spectrometer (ICP) at King's College, London. Further details of this method are in Walsh *et al.* (1981).

Sr isotope analyses were determined at Oxford University using the V.G. Micromass 30 and Isomass, mass spectrometers. Sr was separated from powdered whole rock samples using conventional dissolution and cation exchange techniques. Rb/Sr ratios were calculated from the XRF data obtained at Leicester.

GEOCHEMISTRY

Preliminary General Comments

The geochemical data of the batholith as a complete unit are presented in Figs. 4 and 5 and Table 2. Fig. 4 shows that the batholith displays a typical

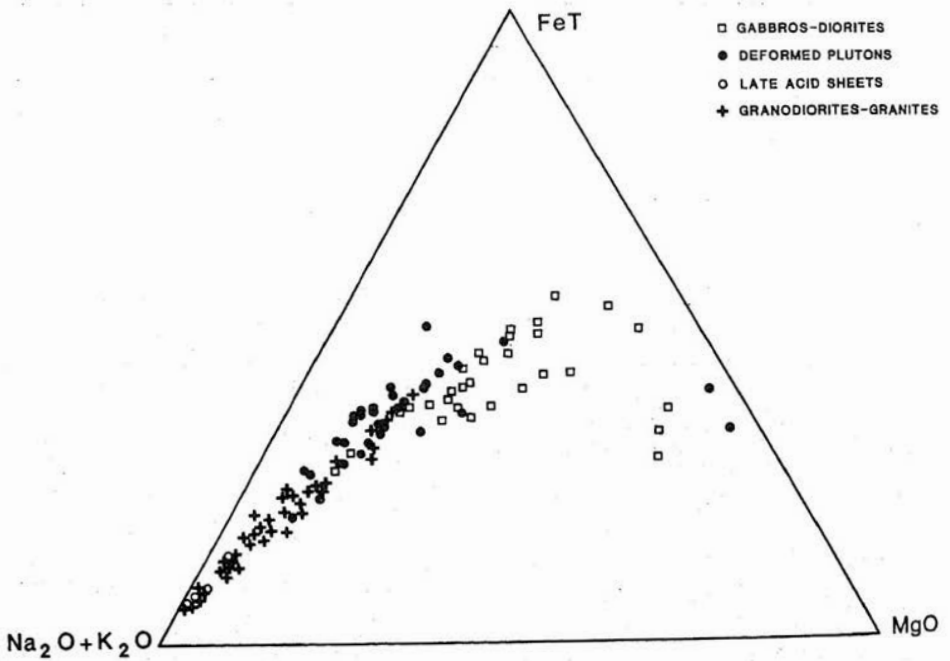

Fig. 4. AFM diagram showing the calc-alkaline character of stages 1, 2 and 3 of the Kohistan batholith.

calc-alkaline trend with respect to the oxides of Na+K, Fe and Mg, and Fig. 5 shows selected trace elements plotted against SiO_2. Element-element plots (Fig. 5) are complex and display a fair degree of scatter about a mean trend. This scatter is caused by (1) the fact that plutonic rocks represent crystal-liquid mushes and not true liquid compositions and (2) many different plutons have been plotted; individual plutons display more constrained magmatic trends.

SiO_2 varies from 42% in the ultrabasic hornblendite rocks to 76% in the leucogranitic rocks. Only K and Rb act incompatibly throughout all compositional ranges, though some elements (Ba, Ce) increase in concentration until minerals with a high KD for these elements start to fractionate at intermediate levels of SiO_2. Other elements, such as Y, Ti, Sr, V act compatibly with respect to SiO_2. These, and other variations, help to elucidate the geochemical evolution of the batholith for each of the three main magmatic stages.

First Stage Deformed Plutons

Figs. 5 and 6 and Table 2 show that the deformed plutonic rocks form two discrete bi-modal geochemical suites which appear to be mutually unrelated. These two suites are: (a) a series of hornblendites, gabbros and diorites (e.g. The North Gilgit Ridge gneiss NGRG (Fig. 6)) which vary in their SiO_2 content from 44% ~ 66% and are characterised by fractionated trace element patterns with high LFS/HFS and LREE/HREE element ratios (Fig. 6). These are geochemically similar to the second stage plutonics — there are however, no equivalents of the second stage high-K granites and leucogranites, or the third stage aplite-pegmatite sheets; (b) a series of quartz-rich high SiO_2 low-K tonalitic gneisses, which have a well constrained, consistent major and trace element composition. Compared to second stage plutons with similar SiO_2 levels they are much less evolved with high MgO, CaO, Fe^T and low Al_2O_3 and K_2O abundances. Their Rare Earth element patterns are unfractionated with $(Ce/Yb)_N$ ratios of circa 1.1, and have low concentrations of Rb, Ba, Sr and LREE. Thus geochemical evidence suggests that they have a different source to the first-stage gabbros-diorites and second stage plutonics. Petterson *et al.* (in prep) have interpreted the low-K gneisses as a partial melt of the Chalt volcanics — petrogenetic modelling shows that this is a possibility, and indicates that partial melting of the immature Kohistan arc crust occurred at an early stage.

Second Stage Undeformed Plutons

This stage of the batholith varies in composition from hornblendite and hornblende gabbro through to granite and more rarely leucogranite (parts of the Shirot pluton). The most modally abundant rock type is granodiorite and the magmatism became progressively more acidic with time.

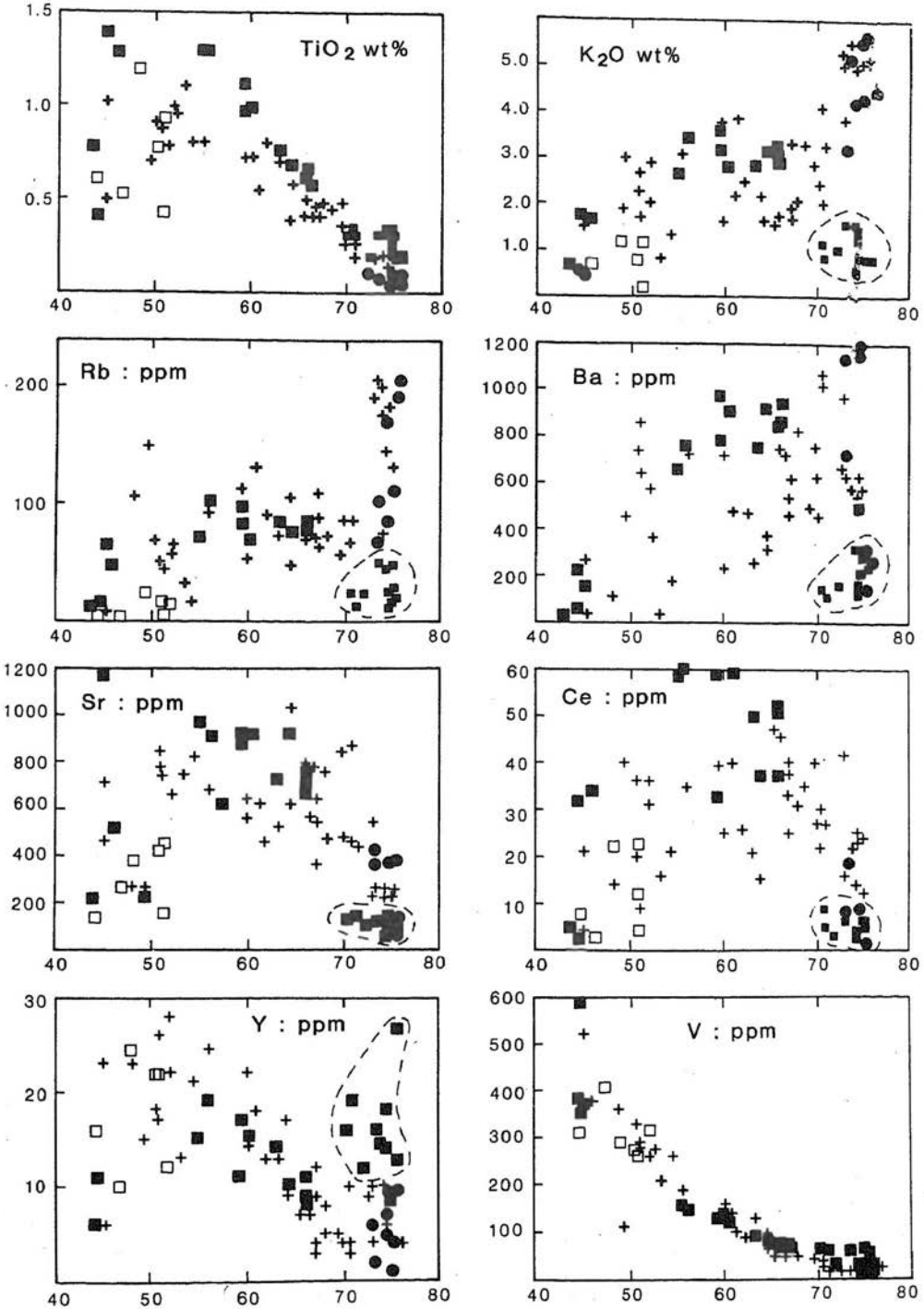

Fig. 5. SiO_2 variation diagrams of plutonic rocks in the batholith.
KEY : Filled square — First Stage Plutonics;
Open square — Second Stage Basic Dykes;
Cross — Second Stage Plutonics;
Filled circle — Third Stage Aplite-Pegmatites.
Field for low K-high SiO_2 tonalites is shown by dashes.

TABLE 2. REPRESENTATIVE WHOLE ROCK XRF ANALYSES.

(1) FIRST-STAGE PLUTONS
A39, A41 — Indus Confluence Tonalite Gneiss.
A144, A149 — Matum Das Tonalite.
P5, A58, A59, A65 — North Gilgit Ridge Gneiss.

(2) BASIC DYKES (SECOND STAGE)
P114 — "Enriched" Dyke.
P121 — "Depleted" Dyke.

(3) SECOND-STAGE GABBROS — DIORITES
P180, P189 — Indus Cofluence Hornblendites.
A54 — Dainyar Diorite.
P201, A204 — Indus Confluence Diorite.
A101 — S. Jutal.
A120 — Sher Qila Diorite.
A127 — Gakuch.

(4) SECOND-STAGE GRANDIORITES — GRANITES
A72 — Gilgit.
A138, A141 — Shirot.
P239 — Jutial.
A124 — Gakuch.
A30 — Bunji.
A4 — Sainallah (10kms S. of Indus Confluence).

(5) THIRD-STAGE APLITE-PEGMATITES
A22, A24 — Parri.
A156, A162 — Indus Confluence.

The major elements follow a typical calc-alkaline trend (Fig. 4) with SiO_2 varying between 45% and 75%, and decreasing FeO^T, MgO, CaO, Al_2O_3, and increasing K_2O+Na_2O with fractionation. Even the most basic gabbros and diorites are enriched in Rb, Ba, K and LREE relative to Zr, Ti, Y and HREE — this geochemical signature is also typical of stage 1 gabbroic diorites. Fig. 7 shows that LREE/HREE and LFS/HFS (e.g. Rb/Ti, K/Y) element ratios increase with fractionation. K and Rb act incompatibly and Sr, Ti, P, V, Cr, Zn and Ni act compatibly with increasing SiO_2. Elements such as La, Ce, Ba and Zr increase in concentration in the basic-intermediate rocks, but decrease in concentration in the more acidic rocks.

These geochemical trends suggest that the ultimate source for the plutonics is an upper mantle source enriched in LFS and LREE elements — low $^{87}Sr/^{86}Sr$ initial ratios support this conclusion (Table 3). Individual plutonic units show evidence of in-situ fractionation — they vary in composition from gabbro to diorite or diorite to granite, and petrographic variations correlate with geochemical variations. Major and trace element modelling (Petterson, 1985), which

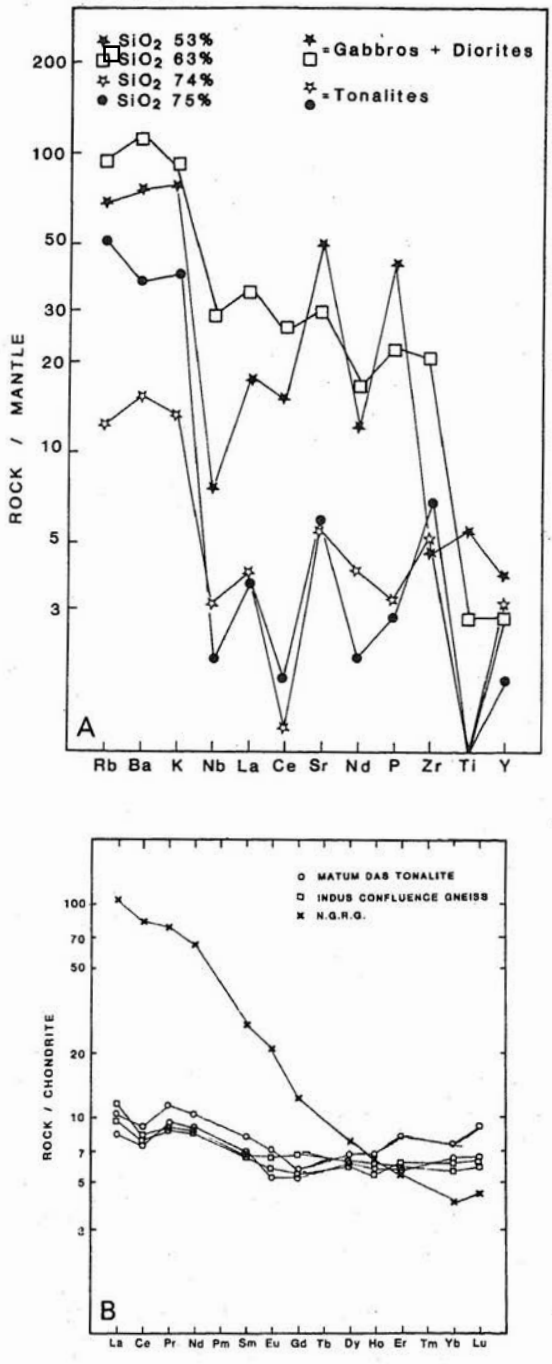

Fig. 6-A. Spidergram variations of trace elements and

6-B. REE diagram of the first stage deformed plutonics NGRG = North Gilgit Gneiss (Gabbroic Diorite).

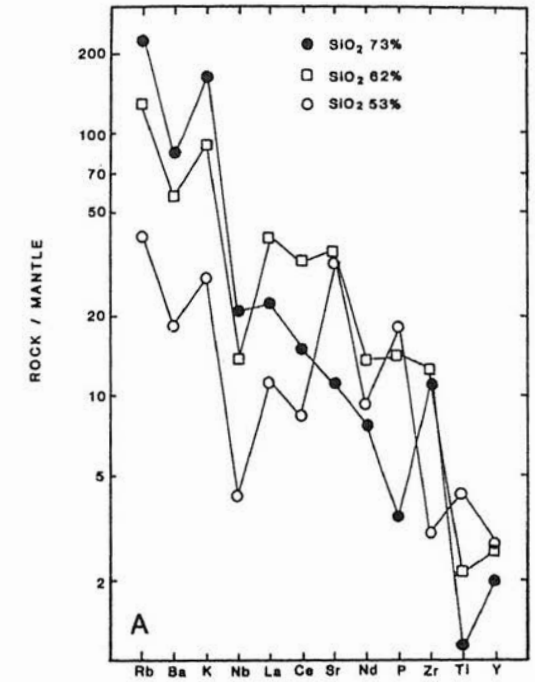

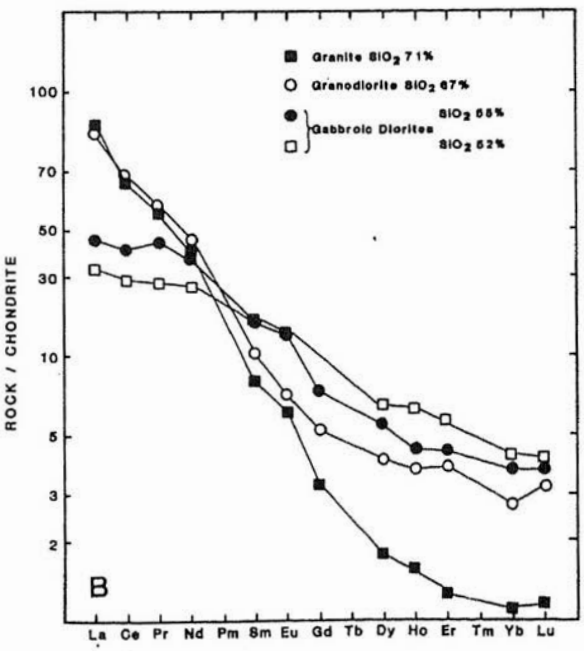

Fig. 7-A. Spidergram variations of trace elements. and

7-B. REE variations in the second stage plutonics.

TABLE 3. $^{87}SR/^{86}SR$ INITIAL RATIO DATA.

Rock Unit	$^{87}Sr/^{86}Sr$ Initial Ration	$^{87}Sr/^{86}Sr$ Present Day
Deformed Tonalite Indus (Confluence)		*0.7048–0.7053
Deformed Tonalite (Matum Das)	0.7039 ± 0.0001	
North Gilgit Ridge Gneiss (Deformed Diorite)		*0.7048–0.7050
Gilgit Granite	0.7041 ± 0.0001	
Shirot Granite	0.7044 ± 0.00006	
Leucogranite, 5 km south of Indus Confluence		*0.7049–0.7051
Indus Confluence Aplite-Pegmatite Sheets.	0.7045 ± 0.00012	
Parri Aplite-Pegmatite Sheets.	0.7052 ± 0.00012	

* Gives the range of present day $^{87}Sr/^{86}Sr$ ratios for analysed samples with varying Rb/Sr ratios.

is beyond the scope of this paper, indicates that hornblende, plagioclase, magnetite-ilmenite ± clinopyroxene were important fractionating phases in the basic-intermediate rocks, and plagioclase, K-feldspar, biotite and magnetite-ilmenite were important fractionating phases in the acid rocks. Minor phases such as sphene, zircon, apatite and allanite removed elements such as La, Ce, Nd, Zr from the melt in intermediate-acid rocks, and K-feldspar fractionation explains the reduction in Ba concentrations in the acid rocks.

Thus the plutons of the second magmatic stage and the gabbroic diorites of the first magmatic stage record a two-stage evolution :

(1) Ultimate derivation by the partial melting of enriched upper mantle and

(2) Subsequent fractionation of the primary magmas during their rise through the mantle/crust and final emplacement.

The Basic Dykes

Table 2 and Fig. 8 illustrate the main features of the hornblende-plagioclase basic dykes. They are basaltic in composition with a SiO_2 content of 50%. However they are divisible on the basis of their chemistry into two groups —

one is enriched in trace elements, especially the low field strength elements relative to a depleted group (Fig. 8, Table 2). The "depleted" group displays a tholeiitic trend on an A–F–M diagram, whereas the "enriched" suite has a calc-alkaline trend. The reasons for the geochemical differences shown by the basic dykes are the subject of a paper in preparation.

The Aplite–Pegmatites

There are three main types of aplite-pegmatite sheets which are distinguishable by fieldwork and geochemistry :

(1) Those which can be related structurally and geochemically to specific plutons such as the Shirot granodiorite and the Gilgit granite (Fig. 2) and which represent the most evolved magmas of those plutons.

(2) A minor series of aplite-pegmatites which intrude meta-sediments 10 km south of Gilgit (the Parri acid sheets in Petterson and Windley, 1985). These are garnet-muscovite pegmatites, which have a consistent composition, and have much lower concentrations of Ba and Sr and higher concentrations of Rb relative to the much more abundant aplite-pegmatite sheets at the Indus Confluence. They also have a higher $^{87}Sr/^{86}Sr$ initial ratio (Table 3).

(3) The Indus Confluence aplite-pegmatites which comprise 90% of all such sheets in the batholith, and which locally make up 30–50% of exposures. Their dominant mineralogy is quartz-alkali feldspar-plagioclase-biotite ± tourmaline. The rocks have a SiO_2 content of 73% and (K_2O + Na_2O) contents of 8%. High concentrations of Sr and Ba (some samples contain up to 1600 ppm Ba and 600 ppm Sr) can be attributed, at least in part, to the presence of cumulus alkali feldspar.

Individual sheets are layered and liquid-liquid contacts between layers are visible in the field. Individual layers have a slightly different composition to other layers, however, they can be related magmatically, either by partial melt or fractionation processes involving alkali feldspar and plagioclase ± biotite as the main fractionating/residual phases.

$^{87}Sr/^{86}Sr$ Initial Ratio Data

The geological implications of the $^{87}Sr/^{86}Sr$ initial ratio data presented in Table 3 were discussed by Petterson and Windley (1985). The full range of present-day $^{87}Sr/^{86}Sr$ ratios is given for plutons which did not yield isochrons;

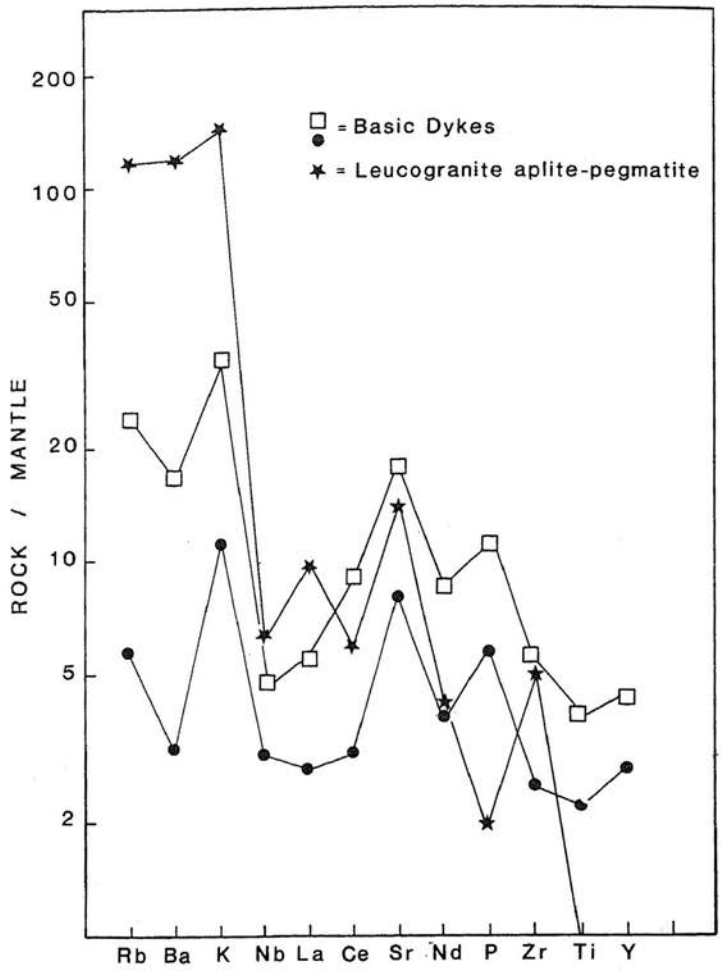

Fig. 8. Spidergram variations of basic dykes and average Indus Confluence aplite-pegmatite composition.

obviously the lower $^{87}Sr/^{86}Sr$ present-day ratios were determined from samples with low Rb/Sr ratios (0.3) and are the closest approximation to the initial $^{87}Sr/^{86}Sr$ ratio.

The low values of $^{87}Sr/^{86}Sr$ initial ratios for all rock units regardless of age or composition (the full range of values only varies from 0.7039–0.7052) suggest that the ultimate source for the plutonics was probably the upper mantle. If any crustal melting did occur, and if this process was responsible for the genesis of the deformed tonalite gneisses, and for the Parri garnet-muscovite leucogranitic sheets, then it must have been crust with a low Rb/Sr ratio and/or a short crustal residence time. This is plausible when it is considered that no

rocks older than Cretaceous have yet been discovered in the Kohistan arc-sequence (Coward *et al.*, 1982, 1986; Petterson and Windley, 1985), and that the deformed tonalite gneisses have an isotopic age = 102 ± 12 Ma.

The range of $^{87}Sr/^{86}Sr$ initial ratios compares with a range of 0.7034–0.7038 for 100–60 Ma intrusives in Ladakh (Honegger *et al.*, 1982). The low initial Sr isotope ratios for the Kohistan leucogranites contrast strongly with the very high initial Sr isotope ratios of between 0.7550 and 0.769 for similar-aged leucogranites south of the Zanskar valley in the Indian plate (Searle and Fryer, 1986). This evidence suggests that the Kohistan leucogranites could not have originated from the partial melting of crystalline Precambrian/Palaeozoic basement, which is the preferred explanation for the origin of the Zanskar leucogranites.

THE ORIGIN AND EVOLUTION OF THE KOHISTAN BATHOLITH

Coward *et al.* (1982, 1986), Petterson and Windley (1985), and Petterson *et al.* (in prep) suggested that the Kohistan belt developed in two major stages.

(1) As an island arc, separated in the north from the Eurasian plate by a marginal back-arc basin, and in the south from the Indian plate by a major ocean which was actively subducting northwards beneath Kohistan.

(2) As an Andean-type margin, after the marginal basin to the north had closed and the Kohistan arc had collided with Eurasia forming the Northern Suture and causing the Jaglot Syncline phase of deformation. Kohistan continued to develop as an Andean margin until subduction ceased after the final major collision between the Indian plate and the Eurasian-Kohistan plate.

The timing of these collisions is extensively discussed by Petterson and Windley (1985). It is worth noting that the Jutal basic dykes which cut the structures associated with the Jaglot syncline are dated at 75 Ma, which gives a lower constraint on the formation of the Northern Suture and the timing of the collision between Kohistan and Eurasia.

Thus the first stage of the batholith which was formed in an island arc environment had ended by 75 Ma. This stage is characterised by (1) The calc-alkaline Chalt volcanic sequence, (2) A series of plutonic rocks ranging in composition from gabbro to leucodiorite. The geochemistry of this plutonic series is typical of many comparable subduction-related plutons (Saunders *et al.*, 1980; Brown, 1982), i.e. even the most basic plutons are enriched in LFS and LREE elements relative to HFS and HREE elements. LFS/HFS and LREE/HREE element ratios increase with increasing SiO_2, and (3) A sequence of low K-high SiO_2 tonalites with flat REE patterns and relatively low abundances of LFS elements. These rocks are most closely related to the Chalt volcanics with respect to their trace element geochemistry and possibly represent a partial melt of this sequence.

	First Stage Deformed Tonalites				First Stage Deformed Hornblendites and Gabbroic Diorites				
Sample No.	A39	A41	A144	A149	A58	P5	A58	A59	A65
SiO_2	75.3	71.68	70.34	73.72	54.98	45.54	54.98	60.21	66.02
TiO_2	0.23	0.33	0.32	0.25	1.3	0.79	1.30	0.98	0.57
Al_2O_3	12.65	12.78	14.59	13.03	17.69	7.38	17.69	18.41	16.54
FeT	1.56	3.79	3.74	3.04	7.72	20.38	7.72	5.93	3.77
MnO	0.03	0.06	0.09	0.07	0.1	0.21	0.1	0.08	0.05
MgO	0.77	1.13	1.16	0.8	3.08	11.19	3.1	2.33	1.49
CaO	3.36	3.85	4.71	3.9	5.91	14.78	5.91	5.18	3.63
Na_2O	3.83	3.4	3.34	3.64	4.34	0.91	4.34	4.57	4.35
K_2O	0.81	1.37	1.15	0.42	2.71	0.77	2.71	2.92	3.25
P_2O_5	0.03	0.05	0.08	0.05	0.66	0.05	0.66	0.5	0.27
Total :	98.57	98.43	99.51	98.92	98.49	99.99	98.49	101.11	99.95
Rb	28	38	23	11	77	10	77	71	82
Ba	221	405	148	120	681	42	681	917	921
Pb	—	—	—	—	—	9	—	—	—
Nb	2	4	1	2	21	1	21	20	15
Sr	160	128	140	137	998	212	998	903	750
Zr	71	66	65	62	290	20	290	271	192
Y	13	14	16	16	15	11	15	15	8

Cr	14	7	7	5	32	21	32	29	26
V	19	72	65	40	158	599	158	123	75
Zn	14	26	36	18	113	63	113	92	60
Ni	3	6	4	4	19	64	19	13	10
La	4	3	4	3	34	1	29	29	22
Ce	7	7	8	7	72	5	63	61	38
Pr	1	1	1	1	9	—	—	—	—
Nd	6	6	7	6	41	4	25	24	16
Sm	1.4	1.4	1.7	1.4	5	—	—	—	—
Eu	0.5	0.5	0.6	0.4	2	—	—	—	—
Gd	1.9	1.5	1.6	1.5	3	—	—	—	—
Dy	2.2	2.1	2.4	2.2	2.7	—	—	—	—
Ho	0.5	0.4	0.5	0.5	0.5	—	—	—	—
Er	1.4	1.4	1.9	1.3	1.2	—	—	—	—
Yb	1.3	1.4	1.7	1.4	0.9	—	—	—	—
Lu	0.19	0.21	0.31	0.22	0.2	—	—	—	—

Second Stage Dyke		Second Stage Granites							
Sample No.	P121	A72	A138	A141	P239	A124	A30	A122	A4
SiO_2	46.64	74.15	71.03	66.95	72.6	69.86	71.08	68.14	73.43
TiO_2	0.52	0.16	0.26	0.41	0.16	0.3	0.31	0.44	0.13
Al_2O_3	18.26	14.1	15.06	15.15	14.33	14.38	14.82	14.72	14.81
FeT	12.22	1.35	2.1	3.52	1.46	2.5	1.94	3.29	1.18
MnO	0.23	0.04	0.03	0.06	0.06	0.07	0.03	0.08	0.02
MgO	6.38	0.3	0.75	1.56	0.33	0.7	0.47	1.75	0.29
CaO	11.78	1.52	2.74	3.86	1.57	2.48	2.22	3.25	2.16
Na_2O	1.92	3.43	3.93	4.17	4.19	3.33	4.1	3.05	4.1
K_2O	0.37	5.002	3.27	1.92	5.33	4.21	3.71	3.28	3.69
P_2O_5	0.05	0.051	0.12	0.13	0.06	0.11	0.11	0.18	0.04
Total :	98.36	100.10	99.3	97.74	100.08	98.00	98.79	98.2	99.90
Rb	4	177	91	65	203	186	80	92	55
Ba	9	565	1081	423	644	678	1459	374	1351
Pb	—	—	—	—	26	—	—	—	—
Nb	1	11	6	8	17	9	6	6	4
Sr	283	245	442	374	261	294	459	424	393
Zr	14	123	167	128	140	136	170	85	91
Y	10	9	4	9	10	17	2	11	4

Cr	62	13	13	40	5	7	14	45	15
V	406	15	33	62	15	37	28	70	10
Zn	97	28	33	45	42	31	42	45	27
Ni	21	4	3	16	—	5	13	19	3
La	1	17	22	24	22	20	15	14	13
Ce	3	32	40	43	42	35	25	24	24
Pr	—	4	4	4	—	—	—	—	3
Nd	3	15	16	17	16	12	7	11	12
Sm	1.5	2	2	2	—	—	—	—	2
Eu	0.52	0.49	0.5	0.6	—	—	—	—	0.6
Gd	—	1.24	0.9	1.5	—	—	—	—	1
Dy	—	1.11	0.6	1.5	—	—	—	—	0.7
Ho	—	0.2	0.1	0.3	—	—	—	—	0.1
Er	1.6	0.5	0.3	0.9	—	—	—	—	0.3
Yb	—	0.5	0.2	0.6	—	—	—	—	0.2
Lu	0.1	01	0.04	0.1	—	—	—	—	0.03

	Second Stage Gabbros — Diorites								Second Stage Dyke
Sample No.	A54	P180	P201	P189	A204	A101	A120	A127	P114
SiO_2	53.08	49.22	57.87	48.09	64.41	54.07	54.84	52.24	51.63
TiO_2	1.1	0.69	0.72	0.63	0.39	0.9	0.52	0.87	1.05
Al_2O_3	17.94	8.92	16.74	10.37	18.12	15.97	18.41	14.9	18.99
FeT	8.66	9.87	6.93	9.49	3.44	8.04	7.88	9.0	9.92
MnO	0.14	0.15	0.14	0.22	0.06	0.13	0.19	0.17	0.19
MgO	7.15	16.7	3.16	16.88	2.06	6.0	4.03	7.39	4.83
CaO	9.32	7.65	6.17	9.19	5.49	8.55	7.16	12.02	8.47
Na_2O	3.34	1.02	3.42	0.47	4.53	3.91	3.77	2.12	3.28
K_2O	0.86	3.01	3.46	3.7	1.61	0.96	3.79	1.79	1.17
P_2O_5	0.38	0.22	0.26	0.24	0.19	0.29	0.41	0.21	0.25
Total :	101.97	97.45	98.87	99.27	100.3	98.82	101.00	100.71	99.78

Rb	35	156	107	257	44	22	64	49	35
Ba	141	454	792	326	317	215	526	435	185
Pb	—	10	4	6	—	—	—	—	7
Nb	2	17	8	12	3	4	2	4	4
Sr	487	246	588	67	610	661	1208	453	440
Zr	40	127	161	59	54	14	48	44	72
Y	13	15	22	29	7	60	19	19	21
Cr	634	1610	22	1540	21	281	27	988	11
V	227	114	152	326	80	203	261	264	240
Zn	76	107	74	128	37	69	87	71	81
Ni	224	609	16	498	20	81	15	48	12
La	10	22	20	12	6	10	18	12	9
Ce	21	48	42	35	15	24	34	19	22
Pr	—	6	5	5	—	—	—	—	3
Nd	11	28	22	27	6	14	16	12	16
Sm	—	4	4	5	—	—	—	—	3
Eu	—	1	1	1	—	—	—	—	1
Gd	—	3	3	5	—	—	—	—	2.7
Dy	—	2.7	3	4.6	—	—	—	—	2.9
Ho	—	0.5	0.6	0.9	—	—	—	—	0.6
Er	—	1.3	2	2.5	—	—	—	—	1.7
Yb	—	1.1	1.7	2.2	—	—	—	—	1.5
Lu	—	0.16	0.12	0.3	—	—	—	—	0.2

THIRD STAGE APLITE-PEGMATITES

Sample No.	A22	A24	A156	A162
SiO_2	73.88	74.76	71.77	75.08
TiO_2	0.07	0.05	0.09	0.05
Al_2O_3	14.28	14.37	15.23	14.47
FeT	1.06	0.73	0.9	0.58
MnO	0.08	0.06	0.02	0.13
MgO	0.1	0.1	0.16	0.1
CaO	1.12	1.11	2.35	1.39
Na_2O	4.36	4.21	4.28	3.41
K_2O	4.27	4.2	3.94	5.64
P_2O_5	0.03	0.02	0.03	0.01
Total :	99.24	99.6	98.78	100.75
Rb	204	193	70	106
Ba	139	181	1568	1036
Pb	—	—	—	—
Nb	11	9	2	2
Sr	82	91	561	371
Zr	33	36	49	26
Y	8	6	1	2
Cr	11	6	8	7
V	3	2	9	6
Zn	47	35	19	13
Ni	3	3	3	3
La	4	4	5	9
Ce	8	8	9	17
Pr	1	1	1	2
Nd	4	4	4.6	9
Sm	1	1	0.6	1.5
Eu	0.2	0.2	0.4	0.5
Gd	1.3	1.5	0.4	0.8
Dy	1.2	0.9	0.5	0.6
Ho	0.2	0.2	0.1	0.1
Er	0.7	0.8	0.3	0.3
Yb	0.5	0.5	0.3	0.3
Lu	0.1	0.2	0.05	0.05

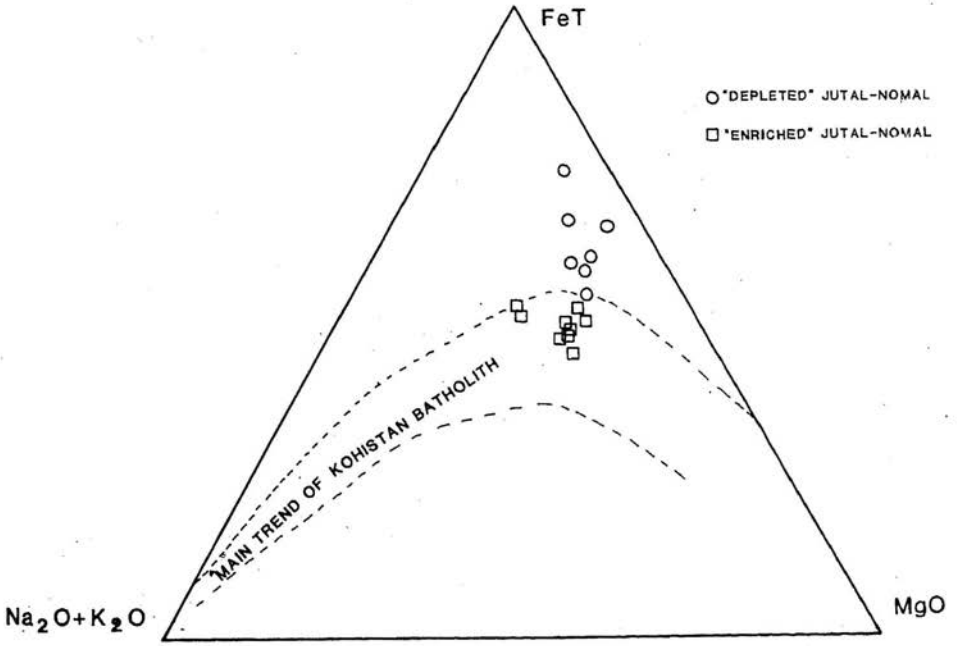

Fig. 9. AFM diagram showing the relationship between the Jutal basic dykes and the main magmatic trend of the arc-batholith.

The second magmatic stage of the batholith was formed at an Andean-type margin. The earliest plutonics of this second stage are the hornblende/plagioclase-bearing basic dykes, gabbros and diorites. Again even the most basic diorites have a geochemistry which is typical of subduction-related magmas. With the progression of time, as the Andean margin became more mature, the magmatism became increasingly acidic, and was able to give rise to typical plutons such as the Gilgit and Shirot granites (Table 2).

Finally, a third stage of magmatism evolved when aplite-pegmatite sheets with leucogranitic compositions were intruded, some of which were probably the product of crustal melting which occurred soon after the terminal collision between India and Eurasia.

Acknowledgements : We thank NERC for a research studentship and Himalayan research grant GR3/4242, and Professors R.A.K. Tahirkheli and M.Q. Jan of Peshawar University for logistical help and much friendly co-operation. M.G. Petterson thanks N. Walsh for the use of ICP equipment at King's College, London University, N. Marsh for assistance with XRF analyses, and we are both grateful to Sue Button for the diagrams. M.G.P. publishes with permission of the Director, British Geological Survey.

REFERENCES

Brookfield, M.I. & Reynolds, P.H., 1981. Late Cretaceous emplacement of the Indus suture zone ophiolitic melanges and an Eocene-Oligocene magmatic arc on the northern edge of the Indian plate. Earth Planet. Sci. Lett. 55, 157—162.

Brown, G.C., 1982. Calc-alkaline intrusive rocks: their diversity, evolution and relation to volcanic arcs. In: (R.S. Thorpe ed.) Andesites: orogenic andesites and related rocks. Wiley, London.

Casnedi, R., Desio, A., Forcella, F., Nicoletti, M. & Petrocianni, C., 1978. Absolute age of some granitoid rocks between Hindu Raj and Gilgit river. Accad. Naz. Lincei Ser. 8, 64, 204—210.

Coward, M.P., Jan, M.Q., Rex, D., Tarney, J., Thirwall. M. & Windley, B.F., 1982. Geotectonic framework of the Himalaya of N. Pakistan. J. Geol. Soc. London 139, 299—308.

Coward, M.P., Windley, B.F., Broughton, R., Luff, I.W., Petterson, M.G., Pudsey, C., Rex, D. & Khan, M.A., 1986. Collision tectonics in the NW Himalayas, In: (M.P. Cowards & A.C. Ries, eds.) Collision Tectonics. Geol. Soc. Lond. Sp. Publ. 19, 203—20.

Debon, F., Le Fort, P., Davtel, D., Sonet, J. & Zimmerman, J.L., 1987. Granites of western Karakorum and Northern Kohistan (Pakistan): A composite Mid-Cretaceous to Upper Cenozoic Magmatism. Lithos. 20, 19—40.

Honegger, K., Dietrich, V., Frank, W., Gansser, A., Thoni, M. & Trommsdorf. V., 1982. Magmatism and metamorphism in the Ladakh Himalayas (The Indus-Tsangpo suture zone). Earth Planet. Sci. Lett. 60, 253—292.

Jan, M.Q. & Howie, R.A., 1981. The mineralogy and geochemistry of the metamorphosed basic and ultrabasic rocks of the Jijal Complex, Kohistan, NW Pakistan, J. Petrol. 22, 85—126.

Jan, M.Q., Khattak, M.U.K., Parvez. M.K. & Windley, B.F., 1984. The Chilas stratiform complex: field and mineralogical aspects. Geol. Bull. Univ. Peshawar 17, 153—169.

Maluski, H., Proust, F. & Xiao, X.C., 1982. $^{39}Ar/^{40}Ar$ dating of the Trans-Himalayan calc-alkaline magmatism of Southern Tibet. Nature 298, 152—154.

Marsh, N.G., Saunders, A.D., Tarney, J. & Dick, H.J.B., 1980. Geochemistry of basalts from the Shikoku and Daito basins, Deep Sea Drilling Project Leg 58. Init. Rep. Deep Sea Drilling Proj. 58, 805—842.

Marsh, N.G., Tarney, J. & Hendry, C., 1983. Trace element geochemistry of basalts from hole 504B, Panama basin, Deep Sea Drilling Projects Legs 69 and 70. Init. Rep. Deep Sea Drilling Proj. 69, 747—763.

Petterson, M.G., 1985. The structure, petrology and geochemistry of the Kohistan batholith, Gilgit, Kashmir, N. Pakistan. Thesis Ph.D. (unpubl.), Univ. Leicester.

Petterson, M.G. & Windley, B.F., 1985. Rb-Sr dating of the Kohistan arc-batholith in the Trans-Himalaya of north Pakistan, and tectonic implications. Earth Planet. Sci. Lett. 74, 45—57.

Petterson, M.G., Saunders, A., Luff, I.W., Windley, B.F. & Rex, D. In prep. The Kohistan Arc Batholith: A Case Study in the multi-stage genesis and evolution of the continental crust.

Pudsey, C.J., Coward, M.P., Luff, I.W., Shackleton, R.M., Windley, B.F. & Jan, M.Q., 1985. The collision zone between the Kohistan arc and the Asian plate in NW Pakistan. Trans. R. Soc. Edinb. 76, 464—479.

Pudsey, C.J., Schroeder, R. & Skelton, P.M., 1985. Cretaceous (Aptian/Albian) age for island arc volcanics, Kohistan, N. Pakistan. In: (Gupta V.J. ed.) Geology of Western Himalayas: Contrbutions to Himalayan Geology 3, 150—168.

Reynolds, P.H., Brookfield, M.E. & McNutt, R.H., 1983. The age and nature of Mesozoic-Tertiary magmatism across the Indus Suture. Geol. Rund. 72, 981—1104.

Saunders, A.D., Tarney, J. & Weaver, S.D., 1980. Traverse geochemical variations across the Antarctic Peninsula: implications for the genesis of calc-alkaline magmas. Earth Planet. Sci. Lett. 46, 344—360.

Scharer, U., Hamet, J. & Allegre, C.J., 1984. The Transhimalaya (Gangdese) plutonism in the Ladakh region: a U-Pb and Rb-Sr study. Earth Planet. Sci. Lett. 67, 327—339.

Searle, M.P., 1983. Stratigraphy, structure and evolution of the Tibetan-Tethys zone in Zanskar and the Indus suture zone in the Ladakh Himalaya. Trans. Roy. Soc. Edinb. 73, 205—219.

Searle, M.P., & Fryer, B.J., 1986. Garnet, tourmaline and muscovite-bearing leucogranites of the High Himalaya from Zanskar, Kulu, Lahoul and Kashmir. In: (M.P. Coward & A.C. Ries, eds.) Collision Tectonics. Geol. Soc. Lond. Sp. Publ. 19, 185—202.

Walsh, J.N., Buckley, F. & Barker, J., 1981. The simultaneous determination of the rare-earth elements in rocks using inductively coupled plasma source spectrometry. Chem. Geol. 33, 141—153.